Magnetic circular dichroism of zinc-blende-phase MnTe

K. Ando, K. Takahashi,* and T. Okuda†
Electrotechnical Laboratory, Tsukuba Science City, Ibaraki 305, Japan

M. Umehara
National Institute for Research in Inorganic Materials, Tsukuba Science City, Ibaraki 305, Japan
(Received 3 February 1992; revised manuscript received 15 June 1992)

Temperature dependence of the magneto-optic effect, i.e., magnetic-circular-dichroism (MCD) spectra, of metastable zinc-blende MnTe films has been investigated. MCD peaks from the Γ point of the Brillouin zone as well as from the Mn *d-d* intra-atomic tranistions were observed. Below 70 K the energy of the Γ peak showed a distinct magnetic blueshift accompanying a rapid increase of the MCD intensity. These anomalies reflect the first-order phase transition into the type-III antiferromagnetic-ordering state of a frustrated Heisenberg antiferromagnet. In the antiferromagnetic-ordering state, a larger magneto-optic effects as compared with that in the paramagnetic state was observed. This large magneto-optic effect in the antiferromagnetic-ordering state is related with the sharpening of the optical-absorption spectra.

I. INTRODUCTION

There has been much recent interest in diluted magnetic semiconductors[1] (DMS) both for study of optical and magnetic effects, as well as for optoelectronic-device possibilities. In DMS the band electrons and holes strongly interact with the localized magnetic moment, and causes a variety of interesting phenomena, such as the giant magneto-optic effect.[2]

The $Cd_{1-x}Mn_xTe$ system is a typical DMS system. It can be considered as a mixed crystal system between two zinc-blende (ZB) phase materials, CdTe and MnTe. Magnetic and optical properties of these base materials are indispensable for the investigation of the $Cd_{1-x}Mn_xTe$ system. CdTe is a well-known nonmagnetic semiconductor. On the contrary, the properties of the zinc-blende phase MnTe have not been clarified because it had been considered to be a hypothetical material until Durbin *et al.*[3] recently succeeded to grow its single-crystal films by a molecular-beam epitaxy. Only theoretical calculations on its electronic structure had been reported.[4–6]

In addition to the importance of ZB MnTe as a base material for the $Cd_{1-x}Mn_xTe$ system, it has also attracted basic interest for its possible unique magnetic behavior.[7,8] Manganese ions in the ZB phase MnTe form a fcc lattice, and interact with their nearest neighbors via antiferromagnetic (AFM) interaction. Such system has no stable magnetic ground state[9] and is called a frustrated Heisenberg antiferromagnet. If one takes into account the next-nearest-neighbor (NNN) magnetic interaction J_{NNN} in addition to the antiferromagnetic nearest-neighbor (NN) interaction J_{NN}, a variety of magnetic ordering can be possible depending on values of J_{NN} and J_{NNN}. In $Cd_{1-x}Mn_xTe$ systems J_{NNN} is also antiferromagnetic and is about one order smaller than J_{NN}.[4] Under this condition, an antiferromagnetic ordering of type three (AFM-III) should be the ground state.[10] The symmetry arguments predict the first-order phase transition between the paramagnetic state and the AFM-III ordering state.[11] In the $Cd_{1-x}Mn_xTe$ system the antiferromagnetic ordering has not been observed up to $x=0.77$, which can be fabricated as bulk crystals.[1] Recently Ando *et al.* grew the 2-μm-thick [111]-oriented ZB-MnTe films and measured its magnetic susceptibility.[12] Their data indicated an antiferromagnetic phase transition at $T\sim 60$ K. Klosowski *et al.*[13] showed a first-order phase transition at $T\sim 70$ K by measuring neutron scattering of the [001]-oriented MnTe films.

In this paper we report the magneto-optical effect on the ZB MnTe. Magneto-optic effects in DMS arise mainly from the optical transition between the Zeeman-splitted Γ_6 conduction-band edge and the Γ_8 valence-band edge. Magneto-optic studies have been reported by many authors,[2,14–16] but in most of these works direct observation of the magneto-optic effect in the vicinity of the band-gap energy have been difficult because of the large optical-absorption coefficient near the band gap. By using thin-film crystals, we succeeded in observing the magneto-optic effect near the band gap. As a magneto-optic effect we measured the magnetic-circular-dichroism (MCD) effect by applying the magnetic field along the light propagation direction (Faraday configuration). MCD is the magnetic-field-induced difference between the optical-absorption coefficients for the two circular polarization. Most papers on magneto-optic effects of DMS measured the rotation of the polarization plane, that is the Faraday effect. The MCD effect and the Faraday effect are related to each other by the Kramers-Kronig relations, and give essentially identical information on the electronic state of materials. However MCD is more suitable to investigate the origin of the magneto-optic effect of the material because the MCD signal is more directly related with the responsible optical transition.

II. EXPERIMENTS

A. Film growth

The samples were fabricated by the ionized cluster-beam method on [0001]-oriented sapphire substrates.[16] Pure ZB phase [111]-oriented MnTe films were obtained at a substrate temperature of 300 °C by using a buffer layer of [111]-oriented CdTe of typical thicknesses of 500 or 1000 A. A trace of the stable phase of MnTe, i.e., NiAs structure, was not detected by the x-ray-diffraction measurement. The lattice constant determined from the x-ray-diffraction peak was 6.34 A, which agreed with the expected lattice constant for ZB MnTe. Thicknesses of the MnTe films used in this study ranged from 1000 to 5000 A. Usage of the transparent sapphire substrates enabled us to observe the magneto-optic effect of MnTe films in a transmission configuration.

B. Magnetic circular dichroism

When a magnetic field is not applied, the transmitted light intensity can be expressed as

$$I=I_0\exp[-k(E)L]\ , \tag{1}$$

where $k(E)$ is the optical-absorption coefficient at energy E without applied magnetic field, L is the thickness of the sample, and I_0 is the input light intensity.

Magnetic field causes the Zeeman splitting of the energy levels. The $\Gamma_8(J=\frac{3}{2})$ valence band splits into four levels, and the $\Gamma_6(J=\frac{1}{2})$ conduction band splits into two levels. For the σ_+ polarized light the $\Gamma_8(J_z=-\frac{3}{2})\rightarrow\Gamma_6(J_z=-\frac{1}{2})$ transition and the $\Gamma_8(J_z=-\frac{1}{2})\rightarrow\Gamma_6(J_z=\frac{1}{2})$ transition are allowed. For the σ_- polarized light the $\Gamma_8(J_z=\frac{3}{2})\rightarrow\Gamma_6(J_z=\frac{1}{2})$ transition and the $\Gamma_8(J_z=\frac{1}{2})\rightarrow\Gamma_6(J_z=-\frac{1}{2})$ transition are allowed. The difference between the optical-absorption coefficients for the two circular polarization causes the MCD effect. But the contributions from $\Gamma_8(J_z=\frac{1}{2})\rightarrow\Gamma_6(J_z=-\frac{1}{2})$ and $\Gamma_8(J_z=-\frac{1}{2})\rightarrow\Gamma_6(J_z=\frac{1}{2})$ transitions to the MCD effect are very small because their intensity are about three times weaker than the others and their energy splitting is much smaller than that for the others.[17,18] We neglect these weak components in the following analysis.

Under these conditions the absorption coefficients k_+ and k_- for the σ_+ and σ_- polarization can be expressed by

$$k_+(E)=k\left[E+\frac{\Delta E}{2}\right] \tag{2}$$

and

$$k_-(E)=k\left[E-\frac{\Delta E}{2}\right]\ , \tag{3}$$

where ΔE is the Zeeman-splitting energy which is expressed as[19]

$$\Delta E=-\langle S^z\rangle N_0(\alpha-\beta) \tag{4}$$

in the first-order perturbation treatment of the sp-d interaction. $\langle S^z\rangle$ is the average spin per Mn ion, N_0 is the number of cation per unit volume. α and β are the integrals of the sp-d exchange interaction for the Γ_6 conduction and Γ_8 valence bands, respectively.

MCD θ per unit light propagation distance expressed in degree units is given by

$$\theta=\frac{180}{4\pi}(k_--k_+)\ . \tag{5}$$

By substituting Eqs. (2) and (3) into Eq. (5), we obtain a following expression:

$$\theta(E)=-\frac{180}{4\pi}\Delta E\frac{dk(E)}{dE}\ . \tag{6}$$

Equation (6) shows the MCD is proportional not only to the Zeeman-splitting energy ΔE but also to the energy derivative of the light-absorption coefficient dk/dE. The energy derivative of the absorption coefficient is known to be a useful quantity to analyze the electronic structure of semiconducting materials. Therefore Eq. (6) shows that MCD measurement is also a useful method in studying the semiconducting materials, especially, for DMS which shows a very large ΔE. Equation (6) also shows that the value of ΔE can be deduced from combined measurements of MCD and absorption spectra. For $Cd_{1-x}Mn_xTe$ with low-Mn concentration, values of ΔE thus determined[20] well agree with the previously reported values by the magnetoreflection spectroscopy method,[21] indicating the applicability of Eq. (6).

MCD and the absorption coefficient were measured by using monochromatic light from a Xe lamp in a spectrum range from 200 to 750 nm. For MCD measurements, the state of the polarization of input light was modulated between the σ_+ and σ_- polarization with 50 kHz by a photoelastic modulator. The transmitted light was detected by a photomultiplier tube and a lock-in amplifier. The temperature of the samples were controlled from 15 to 300 K by using a closed-cycle He gas refrigerator. Magnetic field up to 12 kG was applied along the light propagation direction.

III. RESULTS

Figure 1 shows the MCD spectra at 15 and 50 K. The MCD signal increased linearly with applied magnetic field at all investigated temperature. The noisy signal above 3.8 eV is due to the low transmitted light intensity by the strong interband optical absorption.

The MCD signal is composed of several structures. We attribute a pair of negative large peaks at 3.38 eV and positive weak peaks at 3.6 eV to the $\Gamma_8\rightarrow\Gamma_6$ optical transition at the Γ point of the Brillouin zone on the basis of the compositional dependence of the MCD peaks in the $Cd_{1-x}Mn_xTe$ system[20] which showed a good agreement between the energy of the negative MCD peak and the reported band-gap energy in this system.[22] Our result indicates that the band gap of ZB MnTe is about 3.38 eV at $T=15$ K.

The peak value of the MCD spectrum at 15 K was $-1.7°$ /cm G at 3.38 eV, which is almost as large as the peak value observed in $Cd_{0.8}Mn_{0.2}Te$ samples. The width

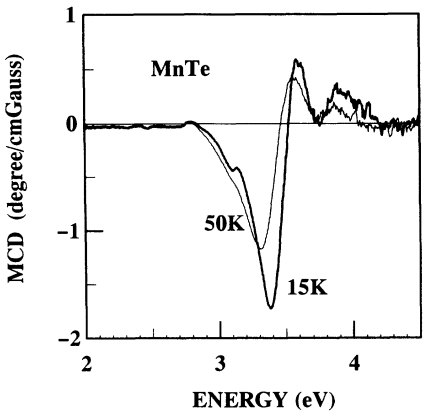

FIG. 1. Photon energy dependence of MCD in MnTe at $T=15$ and $T=50$ K.

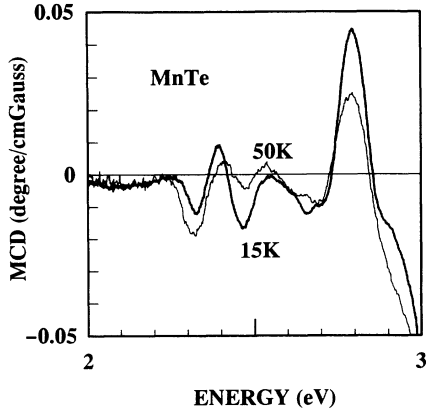

FIG. 2. MCD spectra of MnTe at $T=15$ and 50 K for below 3-eV photon energy.

of the MCD peak was 220 meV, which is about three times wider than that of $Cd_{0.8}Mn_{0.2}Te$. At present it is not clear whether this wide peak shows the intrinsic width or imperfection of the sample.

A positive peak structure around 3.9 eV did not show a noticeable dependence on the sample quality whereas the peak attributed to the $\Gamma_8 \rightarrow \Gamma_6$ optical transition showed a sensitive dependence on the film quality. This indicates that the peak is not related to the $\Gamma_8 \rightarrow \Gamma_6$ optical transition. There are two possible optical transitions responsible for this peak; the L-point optical transition and the spin-orbit splitted $\Gamma_7 \rightarrow \Gamma_6$ optical transition. Kendelewicz[23] estimated the L-point energy of ZB MnTe to be about 3.8 eV based on their manganese concentration dependence of the reflectivity spectra of $Hg_{1-x}Mn_xTe$. On the other hand, Wei and Zunger[6] theoretically calculated the spin-orbit splitting of ZB MnTe to be 0.63 eV. If this spin-orbit-splitting energy is correct, the $\Gamma_7 \rightarrow \Gamma_6$ optical-transition energy should be about 4 eV. Further study is needed for a clear assignment of this peak.

Small but not negligible peaks were also noticed at 3.1 eV and below 3 eV (Figs. 1 and 2). When the temperature changed between 15 and 100 K, these small peaks did not show noticeable energy shift (less than 20 meV), which was in a striking contrast with a large energy shift of the $\Gamma_8 \rightarrow \Gamma_6$ peak (220 meV). This suggests that the origin of these small MCD peaks are of localized nature. We attribute the weak MCD signals to the localized intra-atomic d-d transition in Mn ions. In $Cd_{1-x}Mn_xTe$ systems a clear assignment of Mn intra-atomic transition levels has not been established. Benecke, Busse, and Gumlich[24] tentatively assigned the observed bands of their excitation spectra of luminescence to the transitions from the ${}^6A_1({}^6S)$ ground state to ${}^4T_1({}^4G)$(2.23 eV), ${}^4T_2({}^4G)$($\sim$2.46 eV), and ${}^4A_1{}^4E({}^4G)$(2.6 eV). Other Mn-related optical transitions at a higher-energy range have not been observed because of the small band-gap energy of $Cd_{1-x}Mn_xTe$ crystals which can be obtained as bulk crystals. Among many II-Mn-VI DMS systems, Mn-related optical transitions in $Zn_{1-x}Mn_xS$ systems have been extensively studied because of its wide band-gap energy. In addition to ${}^6A_1({}^6S) \rightarrow {}^4T_1({}^4G)$(2.34 eV), ${}^4T_2({}^4G)$(2.52 eV), and ${}^4A_1{}^4E({}^4G)$(2.68 eV) transitions, the ${}^6A_1({}^6S) \rightarrow {}^4T_2({}^4D)$(2.29 eV) transition and fifth band at 3.16 eV were reported.[24] Overall correspondences between these reported energy of Mn intra-atomic transitions in DMS systems and the energy of observed small MCD signals support our assignments of the observed small MCD peaks to the intra-atomic transitions. The magneto-optic effect of the localized d-d transitions in DMS systems has not been reported so far. The high sensitivity of the polarization modulation method enabled the observation of the magneto-optics of the localized transition.

Figure 3 shows the temperature dependence of the negative peak energy of the MCD peak attributed to the $\Gamma_8 \rightarrow \Gamma_6$ optical transition. With decreasing temperature, the peak energy showed a blueshift. Below $T \sim 70$ K a further blueshift was clearly observed. The blueshift at $T > 100$ K is normal blueshift which is also observed in usual nonmagnetic semiconductors. The large extra blueshift at low temperature should reflect the appearance of the magnetic ordering of ZB MnTe because its magnetic susceptibility indicated the phase transition from the paramagnetic to the antiferromagnetic state at $T \sim 60$

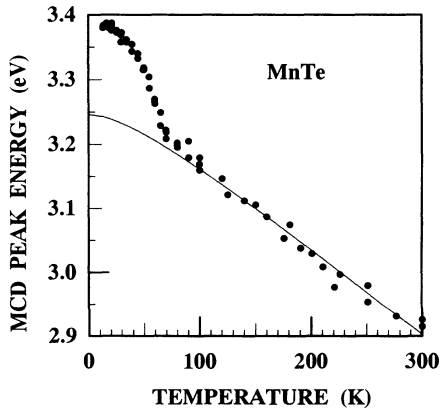

FIG. 3. Temperature dependence of the photon energy E_{MCD} of the negative $\Gamma_8 \rightarrow \Gamma_6$ MCD peak of MnTe. Extrapolated value from data at $T > 100$ K is shown by a solid curve.

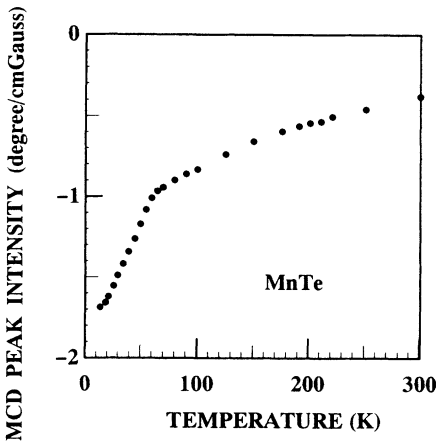

FIG. 4. Temperature dependence of the peak intensity of the negative $\Gamma_8 \rightarrow \Gamma_6$ MCD peak of MnTe.

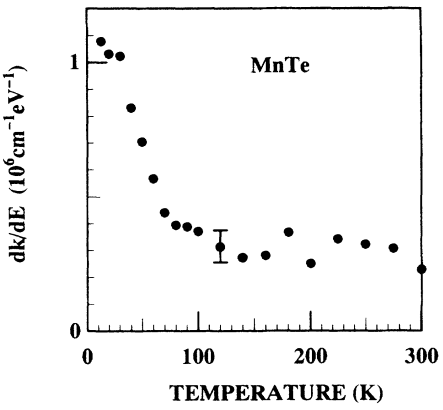

FIG. 6. Temperature dependence dk/dE at the MCD peak energy.

K.[12] In magnetic semiconductors the blueshift of the band-gap energy may be known to correspond to the antiferromagnetic ordering.[25] The experimentally observed blueshift also supports the existence of the anitferromagnetic phase transition in ZB MnTe.

The blueshift of the band-gap energy has been reported in $Cd_{1-x}Mn_xTe$ systems.[26,27] But clear observation of the magnetic blueshift has been very difficulty because of the mixed crystal effect and the difficult of precise determination of the band-gap energy by a conventional optical-absorption spectroscopy.

Figure 4 shows a temperature dependence of the MCD peak intensity. The $\Gamma_8 \rightarrow \Gamma_6$ MCD peak always remained negative irrespective to the temperature. Absolute value of the MCD peak intensity increased with deceasing temperature. Corresponding to the magnetic blueshift, the MCD peak became larger at lower temperature.

As shown by Eq. (6), the MCD is related to the energy derivative of the optical-absorption coefficient, dk/dE. This correspondence is apparent in Fig. 5. The reason of the discrepancy in the higher-energy side of the peaks is not clear now. Figure 6 shows the temperature dependence of dk/dE at the MCD peak energy. Rapid increase of dk/dE in the antiferromagnetic phase corresponds to that of the MCD peak intensity shown in Fig. 4.

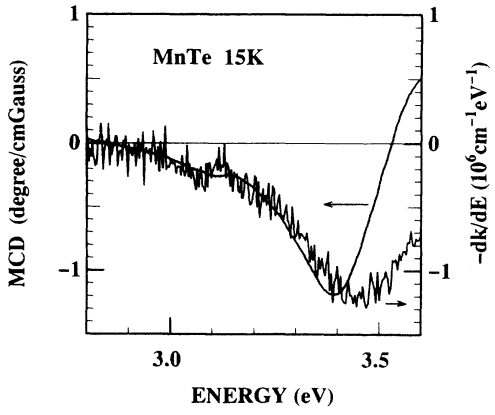

FIG. 5. Spectra of MCD and the energy derivative of the optical-absorption coefficient k.

IV. DISCUSSION

We analyzed the temperature dependence of MCD peak energy E_{MCD} (Fig. 3) at a temperature higher than 100 K by an empirical equation given by Varshni:[28]

$$E(T)=E(0)-\frac{aT^2}{T+b} . \tag{7}$$

The parameter b was fixed to be 65.4 K which explained the temperature dependence of the band gap in CdTe. From a least-square-error fitting analysis we determined the values of the parameters as $E(0)=3.256$ eV and $a=1.45$ meV/K. The fitted curve is shown in Fig. 3 by a solid line. The magnetic blueshift was calculated by subtracting $E(T)$ given by Eq. (7) from the experimental data of E_{MCD} (Fig. 7).

In $Cd_{1-x}Mn_xTe$ the magnetic blueshift of the absorption edge at low temperature was reported to be about 15 and 70 meV for $x=0.3$ and 0.7, respectively.[27] Diouri, Lascarais, and Amrani[26] theoretically calculated the magnetic blueshift by considering the sp-d exchange interaction up to the second-order perturbation and obtained an expression of the compositional dependence of the magnetic blueshift as x^2V/Nq_{max}. V/N is the volume per cation and q_{max} is the cutoff wave vector which is inversely proportional to the lattice constant. If we take account of this compositional dependence, the observed magnetic blueshift of about 145 meV in MnTe was consistent with the data for $Cd_{1-x}Mn_xTe$ ($X<0.7$). In Diouri's model, values of the sp-d interaction integrals α and β were assumed to be independent on Mn concentration. This implies that α and β of ZB MnTe are not so different from the reported values for $Cd_{1-x}Mn_xTe$, i.e., $N_0\alpha=0.22$ eV and $N_0\beta=-0.88$ eV.[1]

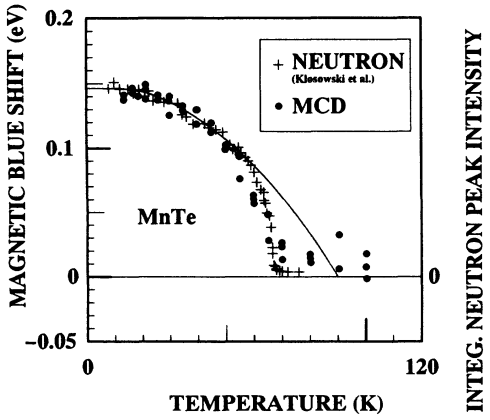

FIG. 7. Magnetic blueshift of the E_{MCD} vs temperature. The solid curve is a squared Brillouin function $B_{5/2}$ with the Curie temperature $T_C = 90$ K. Temperature dependence of integrated neutron peak intensity observed by Klosowski *et al.* (Ref. 13) is also shown for comparison.

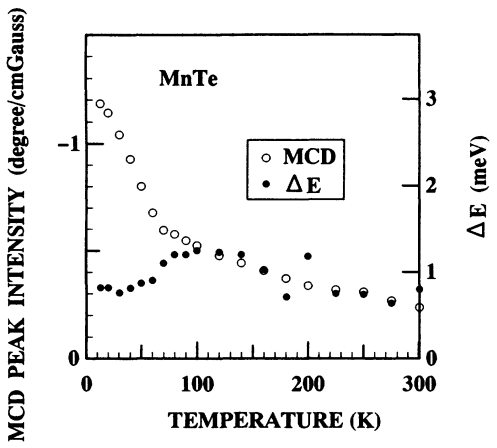

FIG. 8. Temperature dependences of MCD peak intensity and the estimated Zeeman-splitting energy ΔE with $H = 10$ kG for the $\Gamma_8 \rightarrow \Gamma_6$ optical transitions of MnTe.

The magnetic blueshift of the absorption edge in antiferromagnetic semiconductors comes from the second-order perturbation effect of the *sp-d* interaction. Theoretical considerations show that the temperature dependence of the magnetic blueshift can be well expressed by the squared sublattice moment (see Appendix). The superconducting quantum interference device measurement of the magnetic susceptibility indicated the existence of the phase transition at $T \sim 60$ K.[12] However we failed to explain the temperature dependence of the magnetic blueshift by the squared Brillouin function as long as we fixed the Curie temperature to around 60 K. Then we tried to fit the experimental data at the low-temperature region by changing the value of the Curie temperature and obtained a result shown in Fig. 7 by a solid curve. This shows that *Curie temperature* for the second-order transition is about 90 K. The difference between the squared Brillouin function and the experimental data may reflect the first-order phase transition at around 60 K. These findings are in good agreement with the theoretical expectation of the first-order antiferromagnetic phase transition,[7] and are strongly supported by the correspondence between temperature dependence of the magnetic absorption shift and the squared sublattice magnetization of ZB MnTe obtained by the recent results of the neutron scattering (see Fig. 7).[13]

The above discussions show that anomalies observed in the temperature dependences of the MCD of ZB MnTe around 60 K comes from the first-order phase transition between paramagnetic and the type-III anitferromagnetic-ordering state. However the increase of the MCD intensity in the antiferromagnetic-ordering state looks peculiar. Equation (6) shows that MCD depends on both of the Zeeman-splitting energy ΔE and the energy derivative of the optical-absorption coefficient dk/dE. The correspondence between the temperature dependences of the MCD peak intensity and dk/dE is obvious in Figs. 4 and 6. This shows the rapid increase of the MCD intensity in the antiferromagnetic-ordering state in MnTe originates from the sharpening of the optical-absorption coefficient in the magnetic-ordering state. Suppression of the spin fluctuation may sharpen the optical-absorption spectra.

We estimated the value of the Zeeman-splitting energy ΔE by using Eq. (6) (Fig. 8). ΔE became smaller in the antiferromagnetic-ordering state as expected, although it had still a large value.

Bartholomew, Furdyna, and Ramdas[15] analyzed the temperature dependence of the Faraday effect in $Cd_{1-x}Mn_xTe$ ($x \leq 0.7$) by assuming the Curie-Weiss-like temperature dependence. We also analyzed our data of MCD peak intensity of MnTe at $T > 100$ K where dk/dE was almost temperature independent. We obtained the magneto-optic Curie-Weiss temperature of -80 K, which differed from the magnetic Curie-Weiss temperature of -530 K determined from the magnetic susceptibility measurement.[12] Values of $N_0\alpha$ and $N_0\beta$ may not change with temperature. Then the above discrepancy indicates that the magneto-optic effect and the Zeeman splitting in ZB MnTe are not proportional to its magnetization. Although its origin is not clear now, the importance of the higher-order correction to calculate ΔE has been pointed out[18,29] even for $Cd_{1-x}Mn_xTe$ with moderate Mn concentration.

V. CONCLUSIONS

Magneto-optic effects of the zinc-blende phase MnTe has been studied by using MCD. MCD peaks from the Γ point of the Brillouin zone as well as the Mn *d-d* intra-atomic transitions were observed. MCD intensity and its peak energy position of the $\Gamma_8 \rightarrow \Gamma_6$ optical transition showed anomalies at around 60 K. An analysis shows that these anomalies reflect a first-order phase transition between the paramagnetic phase and the type-III antiferromagnetic phase. The Zeeman-splitting energy ΔE was estimated from the spectra of the MCD and the optical-absorption coefficient. ΔE decreased in the antiferromagnetic phase, as expected. But the MCD intensity increased in the antiferromagnetic phase due to the shar-

pening of the optical-absorption spectra in the antiferromagnetic-ordering phase.

ACKNOWLEDGMENTS

One of the authors (K.A.) is grateful to Dr. T. Katayama and Dr. Y. Suzuki for their stimulating discussions. He also thanks Dr. K. Tanaka and Dr. S Yoshida for their encouragement.

APPENDIX

The calculation of the absorption edge shift for magnetic semiconductors may be traced back to Rys, Helman, and Baltensperger.[30] The method has been applied recently to a diluted magnetic semiconductor $Cd_{1-x}Mn_xTe$ by Diouri, Lascaray, and Amrani.[26] They studied only the absolute value of the magnetic blueshift between $T=0$ K and temperatures much higher than the Néel temperature, assuming a single conduction band and a single valence band without the spin-orbit interaction. This assumption seems oversimplified for $Cd_{1-x}Mn_xTe$, as shown later. Besides, they did not show the temperature dependence. In this Appendix, we study the temperature dependence of the magnetic absorption shift for zinc-blende structures, and show that zinc-blende MnTe shows a magnetic blueshift well proportional to the square of the sublattice magnetization when the magnetic absorption shift is mainly brought about by the thermal fluctuation effect of localized moments. During optical-absorption processes, electrons and holes are produced in conduction and valence bands, respectively. In magnetic semiconductors, such a small number of electrons and holes strongly interact with localized magnetic moments, and make the bottom (top) of the conduction (valence) band displace. The interaction Hamiltonian is given by

$$H_n^{\rm int}=-\tfrac{1}{2}\sum_m J_n(\mathbf{r}-\mathbf{R}_m)\boldsymbol{\sigma}\cdot\mathbf{S}_m \ , \tag{A1}$$

where $J_n(\mathbf{r}-\mathbf{R}_m)$ is the exchange interaction between electrons and the Mn local moment $\mathbf{S}_m$ ($S=\frac{5}{2}$) for conduction bands ($n=c$) and valence bands ($n=v$), and $\boldsymbol{\sigma}$ is the Pauli matrix for electrons. We begin with the Hamiltonian in the $(\Gamma,J,J_z;\mathbf{k})$ representation, considering the spin-orbit interaction in zinc-blende structure, where Γ is the band character at $\mathbf{k}=0$, J is the total angular moment, J_z is z component of J, and $\mathbf{k}$ is the wave vector of the electron. Then

$$H=H_c+H_v \ , \tag{A2}$$

$$H_c=\sum_\lambda\sum_{\mathbf{k}}\varepsilon_{\lambda c}(\mathbf{k})a^\dagger_{\lambda\mathbf{k}}a_{\lambda\mathbf{k}}-\sum_{\lambda'\lambda}\sum_{\mathbf{k}'\mathbf{k}}C(\lambda',\mathbf{k}';\lambda,\mathbf{k})a^\dagger_{\lambda'\mathbf{k}'}a_{\lambda\mathbf{k}} \ , \tag{A3a}$$

and

$$H_v=\sum_\lambda\sum_{\mathbf{k}}\{-\varepsilon_{\lambda v}(\mathbf{k})\}d^\dagger_{\lambda\mathbf{k}}d_{\lambda\mathbf{k}}+\sum_{\lambda'\lambda}\sum_{\mathbf{k}'\mathbf{k}}V(\lambda,\mathbf{k};\lambda',\mathbf{k}')d^\dagger_{\lambda'\mathbf{k}'}d_{\lambda\mathbf{k}} \ . \tag{A3b}$$

Here H_c is the Hamiltonian for the conduction band and H_v is that for the valence band. In H_c, $a^\dagger_{\lambda\mathbf{k}}$ and $a_{\lambda\mathbf{k}}$ are, respectively, creation and annihilation operators of an electron with wave vector $\mathbf{k}$ in the conduction band $\lambda=(\Gamma_6,J,J_z)$, and $\varepsilon_{\lambda c}(\mathbf{k})$ is the dispersion of the band. The matrix element for the interaction is given as follows:

$$C(\lambda',\mathbf{k}';\lambda,\mathbf{k})=\tfrac{1}{2}\sum_m\langle\Psi_{\lambda'\mathbf{k}'}(\mathbf{r}-\mathbf{R}_m)|J_c(\mathbf{r}-\mathbf{R}_m)\boldsymbol{\sigma}\cdot\mathbf{S}_m|\Psi_{\lambda\mathbf{k}}(\mathbf{r}-\mathbf{R}_m)\rangle e^{i(\mathbf{k}-\mathbf{k}')\mathbf{R}m} \ , \tag{A4a}$$

where $\Psi_{\lambda\mathbf{k}}(\mathbf{r})$ is the Bloch function with the spin-orbit interaction for zinc-blende structure.[31] For Γ_6, $J=\frac{1}{2}$ and J_z is $\pm\frac{1}{2}$. On the other hand, in H_v, $\varepsilon_{\lambda v}(\mathbf{k})$ is the dispersion of the valence band λ, and $d^\dagger_{\lambda\mathbf{k}}$ and $d_{\lambda\mathbf{k}}$ are, respectively, creation and annihilation operators of a hole; we define $d^\dagger_{\lambda\mathbf{k}}=a_{\lambda\mathbf{k}}$, $d_{\lambda\mathbf{k}}=a^\dagger_{\lambda\mathbf{k}}$. Thus the creation operator $d^\dagger_{\lambda\mathbf{k}}$ produces the vacancy of the electron state at $\mathbf{k}$ in the λ valence band. The matrix element for the interaction is

$$V(\lambda,\mathbf{k};\lambda',\mathbf{k}')=\tfrac{1}{2}\sum_m\langle\Psi_{\lambda\mathbf{k}}(\mathbf{r}-\mathbf{R}_m)|J_v(\mathbf{r}-\mathbf{R}_m)\boldsymbol{\sigma}\cdot\mathbf{S}_m|\Psi_{\lambda'\mathbf{k}'}(\mathbf{r}-\mathbf{R}_m)\rangle e^{i(\mathbf{k}'-\mathbf{k})\mathbf{R}m} \tag{A4b}$$

In the Γ_8 band, $J=\frac{3}{2}$, and thus $J_z=\frac{3}{2}$, $\frac{1}{2}$, $-\frac{1}{2}$, and $-\frac{2}{3}$, while for Γ_7, $J=\frac{1}{2}$, and $J_z=\pm\frac{1}{2}$.

Now, we calculate the self-energy for electrons and holes up to the second-order of the exchange interaction, for the absorption process Γ_8 $(J_z=-\frac{3}{2})$ $\rightarrow\Gamma_6(J_z=-\frac{1}{2})$. The first-order correction for the electron is

$$\Delta E_c^{(1)}(\mathbf{k}_0)=C(\lambda_0\mathbf{k}_0;\lambda_0\mathbf{k}_0)=\tfrac{1}{2}J_c(0)(1/N_0)\sum_m\langle S_m^z\rangle \tag{A5}$$

for $\lambda_0=(\Gamma_6,\frac{1}{2},-\frac{1}{2})$, where

$$J_c(\mathbf{k}'-\mathbf{k})=N_0\langle S_{\mathbf{k}}'(\mathbf{r})|J_c(\mathbf{r})|S_{\mathbf{k}}(\mathbf{r})\rangle \tag{A6}$$

with the s-like Bloch function $S_{\mathbf{k}}(\mathbf{r})$, and thus $J_c(0)=N_0\alpha$ with the conventional exchange constant α.[1] Since $\sum_m\langle S_m^z\rangle=0$ for antiferromagnetic orderings, the first-order energy vanishes. This situation is the same for valence holes. Consequently, the energy correction will be given by the second-order perturbation. For the conduction-band electron at $\mathbf{k}_0=0$,

$$\Delta E_c^{(2)}(\mathbf{k}_0)=\sum_{\lambda}\sum_{\mathbf{q}}\frac{|C(\lambda,\mathbf{k}_0+\mathbf{q};\lambda_0,\mathbf{k}_0)|^2}{\varepsilon_{\lambda_0 c}(\mathbf{k}_0)-\varepsilon_{\lambda c}(\mathbf{k}_0+\mathbf{q})}=-\frac{2m_c}{\hbar^2}\sum_{\mathbf{q}}\frac{G_c^{zz}(\mathbf{q})+G_c^{+-}(\mathbf{q})}{\mathbf{q}^2}\ . \tag{A7}$$

In the last equation, the effective-mass approximation for $\varepsilon_{\lambda c}(\mathbf{k})$, the quasistatic approximation for the localized magnetic system,[32] which may be a good approximation for large S, are used, and

$$G_c^{\alpha\beta}(\mathbf{q})=\left[\frac{1}{2N_0}\right]^2\sum_{l}\sum_{m}|J_c(\mathbf{q})|^2e^{i\mathbf{q}(\mathbf{R}1-\mathbf{R}m)}\langle S_1^{\alpha}S_m^{\beta}\rangle\ . \tag{A8}$$

In the similar way, the second-order correction for the hole in the valence band at $\lambda_0=(\Gamma_8,\frac{3}{2},-\frac{3}{2})$ and $\mathbf{k}_0=0$ is obtained as

$$\Delta E_v^{(2)}(\mathbf{k}_0)=\sum_{\lambda}\sum_{\mathbf{q}}\frac{|V(\lambda_0,\mathbf{k}_0;\lambda,\mathbf{k}_0+\mathbf{q})|^2}{-\varepsilon_{\lambda 0 v}(\mathbf{k}_0)+\varepsilon_{\lambda v}(\mathbf{k}_0+\mathbf{q})}=-\frac{2m(\Gamma_8^h)}{\hbar^2}\sum_{\mathbf{q}}\frac{G_v^{zz}(\mathbf{q})}{\mathbf{q}^2}-\frac{2m(\Gamma_8^l)}{\hbar^2}\sum_{\mathbf{q}}\frac{1}{3}\frac{G_v^{-+}(\mathbf{q})}{\mathbf{q}^2}-\frac{2m(\Gamma_7)}{\hbar^2}\sum_{\mathbf{q}}\frac{2}{3}\frac{G_v^{-+}(\mathbf{q})}{\mathbf{q}^2+[2m(\Gamma_7)\Delta/\hbar^2]}\ , \tag{A9}$$

where the first, second, and third terms are, respectively, contributions from $\lambda=(\Gamma_8,\frac{3}{2},-\frac{3}{2})$, $(\Gamma_8,\frac{3}{2},-\frac{1}{2})$, and $(\Gamma_7,\frac{1}{2},-\frac{1}{2})$. Therefore, $m(\Gamma_8^h)$ and $m(\Gamma_8^l)$ mean, respectively, the effective mass of heavy and light holes for the Γ_8 band, and $m(\Gamma_7)$ is the effective mass for the Γ_7 band. Furthermore Δ is the spin-orbit splitting between Γ_8 and Γ_7 bands at $\mathbf{k}=0$, and

$$G_v^{\alpha\beta}(\mathbf{q})=\left[\frac{1}{2N_0}\right]^2\sum_{l}\sum_{m}|J_v(\mathbf{q})|^2e^{i\mathbf{q}(\mathbf{R}m-\mathbf{R}1)}\langle S_1^{\alpha}S_m^{\beta}\rangle\ , \tag{A10}$$

where

$$J_v(\mathbf{k}'-\mathbf{k})=N_0\langle X_{\mathbf{k}'}(\mathbf{r})|J_v(\mathbf{r})|X_{\mathbf{k}}(\mathbf{r})\rangle=N_0\langle Y_{\mathbf{k}'}(\mathbf{r})|J_v(\mathbf{r})|Y_{\mathbf{k}}(\mathbf{r})\rangle \tag{A11}$$

with the p-like Bloch functions $X_{\mathbf{k}}(\mathbf{r})$ and $Y_{\mathbf{k}}(\mathbf{r})$ for the valence band. [For the calculation of the matrix element of Eq. (A4b), see Ref. 31, for example.] Now we decouple the spin-correlation function $\langle S_1^{\alpha}S_m^{\beta}\rangle$ as

$$\langle S_1^{\alpha}S_m^{\beta}\rangle=\langle S_1^{\alpha}\rangle\langle S_m^{\beta}\rangle+\langle(S_1^{\alpha}-\langle S_1^{\alpha}\rangle)(S_m^{\beta}-\langle S_m^{\beta}\rangle)\rangle\ , \tag{A12}$$

where the first term of the right-hand side is called the ordering term, and the second the fluctuation term. For the ordering term, $\langle S_m^z\rangle=\langle S^z\rangle e^{i\mathbf{Q}\cdot\mathbf{R}m}$, where $\mathbf{Q}=(2\pi/a)(\frac{1}{2},1,0)$ is a vector characterizing the antiferromagnetic ordering of zinc-blende MnTe (Ref. 13) (a is the lattice constant for the fcc lattice), while the fluctuation term is treated by the self-correlation approximation hereafter:

$$\langle(S_1^{\alpha}-\langle S_1^{\alpha}\rangle)(S_m^{\beta}-\langle S_m^{\beta}\rangle)\rangle=(\langle S_1^{\alpha}S_m^{\beta}\rangle-\langle S_1^{\alpha}\rangle\langle S_m^{\beta}\rangle)\delta_{1m}\ .$$

By these approximations, the self-energy of electrons, $\Delta E_c^{(2)}$, is reduced to

$$\Delta E_c^{(2)}(\mathbf{k}_0=0)=-\frac{1}{4}\frac{2m_c}{\hbar^2}\sum_{\mathbf{G}}\frac{|J_c(\mathbf{Q}-\mathbf{G})|^2\langle S^z\rangle^2}{(\mathbf{Q}-\mathbf{G})^2}-\frac{1}{4}\frac{2m_c}{\hbar^2}\frac{1}{N_0}\sum_{\mathbf{q}}\frac{|J_c(\mathbf{q})|^2\{S(S+1)-\langle S^z\rangle^2\}}{\mathbf{q}^2}\ , \tag{A13}$$

where $\mathbf{G}$ is the reciprocal vector for fcc lattice. The first term of $\Delta E_c^{(2)}$ is the contribution from the ordering term, while the second term is that from the fluctuation. Hereafter, $J_c(\mathbf{q})$ and $J_v(\mathbf{q})$ are, respectively, approximated by $J_c(0)=N_0\alpha$ and $J_v(0)=N_0\beta$.[1] Instead, we must impose the cutoff wave vector $q_{\max}$ for the summation over $\mathbf{q}$ or $\mathbf{G}$. It seems reasonable to choose $q_{\max}$ so as to enclose a number of modes equal to the number of magnetic atoms. Then $q_{\max}=(2\pi/a)(\pi/3)^{1/3}=0.984\times(2\pi/a)$, which, however, is a little smaller then $|\mathbf{Q}|=(2\pi/a)(\sqrt{5}/2)=1.11\times(2\pi/a)$. Thus, hereafter, we shall for convenience take $q_{\max}=|\mathbf{Q}|$. Then $\Delta E_c^{(2)}$ is approximated as

$$\Delta E_c^{(2)}=-\frac{1}{4}|J_c(0)|^2(2m_c/\hbar^2q_{\max}^2)\{3\langle S^z\rangle^2+(q_{\max}^3a^3/8\pi^2)[S(S+1)-\langle S^z\rangle^2]\}=\frac{1}{4}\frac{|J_c(0)|^2}{W_c}\{-fS(S+1)+(f-g)\langle S^z\rangle^2\}\ , \tag{A14}$$

where W_c is the bandwidth of the conduction band defined by $z\hbar^2/(2m_ca^2)$ (z is the number of the first nearest neighbor), $f=(q_{\max}az/8\pi^2)=1.067$, $g=(3z/Q^2a^2)=0.729$, and thus $f-g=0.338>0$. The term with g is the contribution from the ordering term [three reciprocal vectors contribute to the first term of Eq. (A13)], and the term with f is that from the fluctuation. The calculation explicitly indicates that the self-energy of electrons at the bottom of the conduc-

tion band causes a blueshift for absorption edge, and its temperature dependence is described by the square of the sublattice magnetization $\langle S^z\rangle^2$ within the self-correlation approximation.

The contribution from the valence-band hole is not so simple as the conduction-band electron, because of the presence of three types of hole effective masses, and the spin-orbit interaction. Using the same approximation as the conduction band, we obtain the self-energy of holes at $\lambda(\Gamma_8, \frac{3}{2}, -\frac{3}{2})$ and $\mathbf{k}_0=0$, as follows:

$$\Delta E_v^{(2)}(\mathbf{k}_0=0)=\frac{1}{4}\frac{|J_v(0)|^2}{W(\Gamma_8^h)}\{-fS(S+1)h-f\langle(S^z)^2\rangle(1-h)+(f-g)\langle S^z\rangle^2\}\ , \tag{A15}$$

with

$$h=\frac{1}{3}\frac{W(\Gamma_8^h)}{W(\Gamma_8^l)}+\frac{2}{3}\frac{W(\Gamma_8^h)}{W(\Gamma_7)}-\frac{2}{3s}\frac{W(\Gamma_8^h)}{W(\Gamma_7)}\left[\frac{\Delta}{W(\Gamma_7)}\right]^{1/2}\tan^{-1}\left[s\left[\frac{W(\Gamma_7)}{\Delta}\right]^{1/2}\right], \tag{A16}$$

where $W(\Gamma_8^h)$, $W(\Gamma_8^l)$, and $W(\Gamma_7)$ are, respectively, the bandwidth for the heavy and light holes in the Γ_8 band, and that for the Γ_7 band, with the same definition as the electron band. Furthermore, $0<h<1$ and $s=(q_{\max}a/\sqrt{z})=2.027$. We can see that the self-energy of holes is a function of both $\langle(S^z)^2\rangle$ and $\langle S^z\rangle^2$. When $f(1-h)\gg(f-g)$, the term with $\langle(S^z)^2\rangle$ is dominant and causes a redshift, while when $(f-g)\gg f(1-h)$, the term with $\langle S^z\rangle^2$ becomes dominant and causes a blueshift. Note that in the limit of $W(\Gamma_8^h)\sim W(\Gamma_8^l)\sim W(\Gamma_7)$ and $\Delta\sim 0$, h approaches to 1.0. In this limit, the situation in the valence-band hole becomes the same as that in the conduction-band electron, which is just the case as treated by Diouri, Lascaray, and Amrani[26] So far the contribution for the optical-absorption edge shift has been separately discussed for electrons and holes, however, the effect of the second order perturbation is sum of the both contribution

$$\Delta E_g^{(2)}=\Delta E_c^{(2)}+\Delta E_v^{(2)}\ . \tag{A17}$$

Now, we remark the following points concerning MnTe: (i) When the contribution from the conduction band is dominant, a blueshift with the temperature dependence of $\langle S^z\rangle^2$ is concluded. On the other hand, when the contribution from the valence hole is dominant, the situation becomes complex, as mentioned above. (ii) In $Cd_{1-x}Mn_xTe$, because both the effective mass and the exchange interaction for the conduction electron are much smaller than those for the valence hole,[1] the main contribution for the magnetic absorption shift comes from the valence hole. The situation may be the same for zinc-blende MnTe. (iii) Judging from the experimental data for $Cd_{1-x}Mn_xTe$,[26] $Cd_{1-x}Mn_xTe$ shows a magnetic blueshift for different concentrations between $0.3<x<0.73$. (iv) According to the present experiment, a magnetic blueshift is also concluded for zinc-blende MnTe. For zinc-blende MnTe, the wave vector indicating the antiferromagnetic ordering $\mathbf{Q}$ is fairly large; for example, $|\mathbf{Q}|=\sqrt{3}\pi/a$ for sc and fcc second type I, while for MnTe, $|\mathbf{Q}|=\sqrt{5}\pi/a$. Furthermore, because the $3d$ wave function of the Mn atom is fairly extended compared with the $4f$ wave function in rare earth, q dependence of the exchange coupling, which may be described as $J(\mathbf{q})\sim J(0)\exp(-u^2\mathbf{q}^2)$, becomes important. (A similar discussion is seen in the paper by Diouri, Lascaray, and Amrani.[26] The ordering term in the second-order perturbation is proportional to $J(|\mathbf{Q}|)^2$ [for example, see the first term of Eq. (A13)], which decreases rapidly for the large $\mathbf{Q}$ for MnTe. Therefore, there is a large possibility that the ordering effect becomes small for zinc-blende MnTe: g may be considerably smaller than 0.729 estimated at the beginning. Moreover when we see that $\langle(S^z)^2\rangle$ is well approximated by $\frac{1}{2}\langle S^z\rangle^2+\frac{1}{3}S(S+1)$ for $S=\frac{5}{2}$,[33] the self-energy of holes, given in Eq. (A15), is further approximated to

$$\frac{|J_v(0)|^2}{4W(\Gamma_8^h)}\{[\tfrac{1}{2}f(1+h)-g]\langle S^z\rangle^2-\frac{1}{3}f(1+2h)S(S+1)\}\ .$$

This evidently shows a magnetic blueshift proportional to $\langle S^z\rangle^2$ for the case of small g. In this way, we can conclude for zinc-blende MnTe that the self-energy correction for both the electrons and holes causes a magnetic blueshift approximately proportional to the square of the sublattice moment when the magnetic absorption shift is mainly brought about by the thermal fluctuation effect of localized magnetic moments. This conclusion is strongly supported by the comparison between the temperature dependence of the absorption shift and the square of the sublattice magnetization of MnTe obtained from neutron studies (see Fig. 7).

So far the thermal fluctuation effect of localized spins has been treated by the self-correlation approximation. Taking into account the correlation between different sites requires the Hamiltonian for localized spins of zinc-blende MnTe which gives rise to a first-order transition. Such a study is deferred to a future study.

Finally, the absolute value of the magnetic blueshift given by

$$\Lambda=\frac{|J_c(0)|^2S^2}{4W_c}(f-g)+\frac{|J_v(0)|^2S^2}{4W(\Gamma_8^h)}[\tfrac{1}{2}f(1+h)-g] \tag{A18}$$

is roughly estimated. Using $m_c=0.1m_e$, $m_v=0.6m_e$,[1] and $a=6.34$ Å, we obtain $W_c=11.4$ eV and $W(\Gamma_8^h)=1.90$ eV. The value of g may be substantially reduced as already discussed, while the fluctuation term (f) is not so reduced since the lower limit of the integral [see the second term of Eq. (A13)] starts from $q=0$. Then as an

example we assume $g=0.35$, which is about half of the value estimated at the beginning, and $f=0.80$. The value of h, also, is not estimated accurately, however, the value may be around 0.5. With $J_c(0)=N_0\alpha\equiv 0.22$ eV, $J_v(0)=N_0\beta=-0.88$ eV,[1] and $S=\frac{5}{2}$, we obtain $\Lambda=0.003+0.159=0.162$ (eV), which compares reasonably well with the experimental value of 0.145 eV. We can see that the magnetic blueshift of zinc-blende MnTe almost comes from the self-energy correction for the valence-band holes.

---

*Permanent address: Nihon Institute of Technology, Saitama, Japan.

†Present address: Nagoya Institute of Technology, Nagoya, Japan.

[1]J. K. Furdyna, J. Appl. Phys. **64**, R29 (1988).

[2]J. A. Gaj, R. R Galazka, and M. Nawrocki, Solid State Commun. **25**, 193 (1978).

[3]S. M. Durbin, J. Han, Sungki O, M. Kobayashi, D. R. Menke, R. L. Gunshor, Q. Fu, N. Pelekanos, A. V. Nurmikko, D. Li, J. Gonsalves, and N. Otsuka, Appl. Phys. Lett. **55**, 2087 (1989).

[4]B. E. Larson, K. C. Hass, H. Ehrenreich, and A. E. Carlsson, Solid State Commun. **56**, 347 (1985).

[5]B. E. Larson, K. C. Hass, H. Ehrenreich, and A. E. Carlsson, Phys. Rev. B **37**, 4137 (1988).

[6]S.-H. Wei and A. Zunger, Phys. Rev. B **35**, 2340 (1987).

[7]T. M. Giebultowicz, J. Magn. Magn. Matter. **54-57**, 1287 (1986).

[8]C. L. Henley, Phys. Rev. Lett. **62**, 2056 (1989).

[9]P. W. Anderson, Phys. Rev. **79**, 705 (1950).

[10]T. M. Giebultowicz and T. M. Holden, in *Semiconductors and Semimetals,* edited by R. K. Willardson, A. C. Beer, J. K. Furdyna, and J. Kossut (Academic, Boston, MA, 1988), Vol. 25, p. 125.

[11]P. Bak and D. Mukamel, Phys. Rev. B **13**, 5086 (1976).

[12]K. Ando, K. Takahashi, and T. Okuda, J. Magn. Magn. Mater. **104-107**, 993 (1992).

[13]P. Klosowski, T. M. Giebultowicz, J. J. Rhyne, N. Samarth, H. Luo, and J. K. Furdyna, J. Appl. Phys. **70**, 6221 (1991).

[14]A. E. Turner, R. L. Gunshor, and S. Datta, Appl. Opt. **22**, 3152 (1983).

[15]D. U. Bartholomew, J. K. Furdyna, and A. K. Ramdas, Phys. Rev. B **34**, 6943 (1986).

[16]T. Koyanagi, K. Matsubara, H. Takaoka, and T. Takagi, J. Appl. Phys. **61**, 3020 (1987).

[17]G. Rebmann, C. Rigaux, G. Bastard, M. Menant, R. Triboulet, and W. Giriat, Physica B+C **117&118B**, 452 (1983).

[18]J. P. Lascaray, D. Coquillat, J. Deportes, and A. K. Bhattacharjee, Phys. Rev. B **38**, 7602 (1988).

[19]J. A. Gaj, J. Ginter, R. R. Galazka, Phys. Status Solidi B **89**, 655 (1978).

[20]K. Ando *et al.* (unpublished).

[21]J. A. Gaj, R. Planel, and G. Fishman, Solid State Commun. **29**, 435 (1979).

[22]Y. R. Lee and A. K. Ramdas, Solid State Commun. **51**, 861 (1984).

[23]T. Kendelewicz, Solid State Commun. **36**, 127 (1980).

[24]C. Benecke, W. Busse, and H.-E. Gumlich, J. Cryst. Growth **101**, 931 (1990).

[25]B. Batlogg, E. Kaldis, A. Schlegel, and P. Wachter, Phys. Rev. B **12**, 3940 (1975).

[26]J. Diouri, J. P. Lascaray, and M. El Amrani, Phys. Rev. B **31**, 7995 (1985).

[27]T. Donofrio, G. Lamarche, and J. C. Woolley, J. Appl. Phys. **57**, 1932 (1985).

[28]Y. P. Varshni, Physica **34**, 149 (1967).

[29]A. K. Bhattacharjee, Solid State Commun. **65**, 275 (1988).

[30]F. Rys, J. S. Helman, and W. Baltensperger, Phys. Kondens. Materie **6**, 105 (1967).

[31]For example, see E. O. Kane, in *Semiconductors and Semimetals,* edited by R. K. Willardson and A. C. Beer (Academic, New York, 1966), Vol. 1, p. 75.

[32]See, for example, P. G. de Gennes and J. Friedel, J. Phys. Chem. Solid **4**, 71 (1958).

[33]The deviation depends on temperature, but is quite small. For example, at $t=T/T_N=0$, $\langle(S^z)^2\rangle=6.25$, while $U=\frac{1}{2}\langle S^z\rangle^2+\frac{1}{3}S(S+1)=6.04$. Furthermore, at $t=0.5$, $\langle(S^z)^2\rangle=5.28$, $U=5.38(\langle S^z\rangle^2=4.93)$, at $t=0.7$, $\langle(S^z)^2\rangle=4.39$, $U=4.62(\langle S^z\rangle^2=3.40)$, and at $t=0.9$, $\langle(S^z)^2\rangle=3.41$, $U=3.56(\langle S^z\rangle^2=1.30)$.